1916 - 2026

An Acad Bras Cienc (2026) 98(Suppl. 1): e20250013 DOI 10.1590/0001-3765202620250013
Anais da Academia Brasileira de Ciências | *Annals of the Brazilian Academy of Sciences*
Printed ISSN 0001-3765 I Online ISSN 1678-2690
www.scielo.br/aabc | www.fb.com/aabcjournal

CHEMICAL SCIENCES

Chemical Profile, Chemometric Analysis, Acetylcholinesterase Inhibitory and Antioxidant Activity of Diverse Boldo Species Employed in The Amazon Region

JOSIELE V. GOMES, ÍVINA T.M. TRINDADE, RAFAELA R. DA SILVA, BRUNA R. DE LIMA, ANDRÉ C. DE OLIVEIRA, FELIPE M.A. DA SILVA & DOMINIQUE F.M. DO CARMO

Abstract: The term 'boldo' is popularly used in the Amazon region to refer to different plant species. This study aimed to identify the chemical profile, evaluate the antioxidant potential and acetylcholinesterase inhibitory activity of leaf infusions of fresh samples of *Plectranthus barbatus*, *Plectranthus ornatus*, *Gymnanthemum amygdalinum*, and *Peumus boldus* commercially acquired at different retail venues in Manaus and Itacoatiara (AM), Brazil. The compounds tentatively identified included the alkaloids *N*-methyllaurotetanine, *N*-methylcoclaurine, isoboldine, and norisoboldine in *P. boldus* leaves; the flavonoid glycosides luteolin 7-*O*-glucoside and quercetin 3-*O*-glucoside, along with diterpenoid coleon H, in *P. ornatus*; the flavonoid glycoside isorhamnetin 3-*O*-glucoside and rosmarinic acid in *P. barbatus*; and the flavonoid glycoside apigenin 7-*O*-glucoside, toguether with 3-*O*-caffeoylquinic acid, in *G. amygdalinum*. The antioxidant activity was assessed using the DPPH assay, with *P. boldus* exhibiting the highest activity among the samples at 1073.33 µM ET. The remaining extracts showed moderate anti-acetylcholinesterase activity. In the *in silico* prediction assay, luteolin 7-*O*-glucoside showed the strongest acetylcholinesterase inhibitory activity, with a binding energy of -10.4 kcal.mol^{-1}. This study enhances the understanding of the chemical and biological knowledge of *P. barbatus*, *P. ornatus*, *G. amygdalinum*, and *P. boldus*.

Key words: medicinal plants, flavonoid glycosides, phenolic compounds, boldo-do-Chile.

INTRODUCTION

In Brazil, the term 'boldo' is popularly employed to refer to different plant species. Among these species are *Plectranthus barbatus* Andrews and *Plectranthus ornatus* Codd, both belonging to the Lamiaceae family, and *Gymnanthemum amygdalinum (Delile) Sch.Bip. ex Walp.* and *Peumus boldus* Molina, which belong to the *Asteraceae* and *Monimiaceae* families, respectively (Schwanz 2006).

The common denomination of these plants arises from their traditional use in the treatment of digestive and hepatobiliary disorders. However, only *P. boldus* —commonly known as 'boldo-do-Chile'—is scientifically validated as true boldo, with numerous studies corroborating its pharmacological properties (Cassels et al. 2019). While the other species are widely adopted as alternatives to *P. boldus* (Costa 2017) due to their ease of cultivation in local Brazilian gardens—ensuring affordability for low-income populations—*P. boldus* remains commercially exclusive, as it relies on imports from Chile.

Notably, the four plant species collectively referred to as 'boldo' belong to distinct botanical families, leading to significant variations in the size and morphology of their vegetative and reproductive structures. Despite these taxonomic and morphological differences, their leaves exhibit comparable traditional medicinal uses, particularly for treating digestive and hepatobiliary disorders (Otero et al. 2022). This pharmacological congruence likely explains their shared vernacular nomenclature (Santos 2022). Furthermore, extensive phytochemical research has revealed these species possess complementary bioactive properties, demonstrating significant antioxidant, anti-inflammatory, antimicrobial, antifungal, and anthelmintic activities (Falé et al. 2009, Costa 2017, Carvalho et al. 2018).

Regarding their principal bioactive constituents, *P. boldus* contains notable compounds including aporphine alkaloids (boldine), phenolic compounds (tannins and catechins) (Hosalkova et al. 2015), coumarins (Fuentes-Barros et al. 2023), and essential oils composed mainly of monoterpenes (Lopes et al. 2020). In contrast, *Plectranthus* species are characterized by terpenoids (especially diterpenes), phenolic compounds (Ishii et al. 2022), and essential oils rich in monoterpenes (Alasbahi & Melzig 2010). *G. amygdalinum* primarily contains flavonoids, tannins, and terpenoid alkaloids (including sesquiterpene lactones, saponins, steroid glycosides, and triterpenoids) (Da Silva et al. 2013), along with essential oils composed mainly of mono- and sesquiterpenes (Usunobun & Ngozi 2016).

A recent phytochemical analysis has revealed a significant flavonoid content across all four boldo species (Da Silva et al. 2022). Notably, both *P. boldus* and *G. amygdalinum* contain substantial quantities of tannins and alkaloids (Falé et al. 2009, Santos 2022). The shared presence of these bioactive compounds likely contributes to their overlapping biological activities. Extensive research has established these phytochemicals as potent free radical scavengers, demonstrating therapeutic potential against oxidative stress-related pathologies (Quezada et al. 2004, Simirgiotis & Schmeda-Hirschmann 2010, Lara-Fernández et al. 2013, Cassels et al. 2019, Fuentes-Barros et al. 2023). Consequently, comprehensive analysis of antioxidant capacity and total phenolic content may elucidate the phytochemical basis for their observed medicinal properties.

Acetylcholine (ACh) plays a crucial role in cognitive function, and its deficiency represents a hallmark feature of Alzheimer's disease (AD). Consequently, acetylcholinesterase (AChE) inhibition has emerged as a key therapeutic strategy for AD management, functioning to elevate synaptic ACh levels and improve cholinergic neurotransmission in affected individuals (Da Silva et al. 2022). Furthermore, growing evidence suggests that oxidative stress, which is both a consequence and driver of AD pathology, significantly contributes to disease progression. This dual mechanism highlights the potential therapeutic value of compounds possessing both AChE inhibitory and antioxidant properties for slowing AD advancement (Da Silva et al. 2022, Carvalho 2014).

Variations in the phytochemical profiles among boldo species may elicit distinct biological effects and potentially adverse reactions. Precise characterization of bioactive compounds in plant-derived infusions is essential to guarantee their safe consumption and prevent potential health risks (Schwanz et al. 2008, Cassels et al. 2019). Comprehensive chemical profiling serves as a critical quality control measure, enabling both the identification of characteristic chemical markers and the detection of potential contaminants or adulterants (Schwanz et al. 2008).

This study sought to identify four boldo species, namely, *P. barbatus*, *P. ornatus*, *G. amygdalinum*, and *P. boldus* commercially available in the municipalities of Manaus and Itacoatiara, investigate their potential antioxidant activity against DPPH, acetylcholinesterase inhibitory and determine their total phenolic content as well as assess the chemical markers of samples marketed as genuine boldo.

The phytochemical profiles of plant species can be characterized using chemometric approaches, particularly Principal Component Analysis (PCA) and Hierarchical Cluster Analysis (HCA). These methods facilitate chemical pattern recognition by clustering samples with similar compositions and identifying discriminant chemical markers (Silva et al. 2016). The present study aimed to authenticate four species commercialized as boldo (*P. barbatus*, *P. ornatus*, *G. amygdalinum*, and *P. boldus*) in the Manaus and Itacoatiara, evaluate their antioxidant potential through DPPH radical scavenging assays, assess acetylcholinesterase inhibitory activity, quantify total phenolic content, and characterize chemical markers in samples marketed as authentic boldo.

MATERIALS AND METHODS

Sample Collection and Preparation

Fresh leaves from mature specimens of *P. barbatus*, *P. ornatus*, and *G. amygdalinum* were collected across multiple locations in Itacoatiara, Amazonas State, Brazil, during August 2022. Commercially available dried leaves of *P. boldus* (marketed as 'boldo-do-Chile') were procured from various retail establishments in both Itacoatiara and Manaus municipalities (Table I).

Aqueous extracts were prepared from each boldo species following standardized infusion protocols. For *P. boldus*, infusions were prepared by adding 10 g of manually crushed dried leaves to 250 mL of boiling distilled water (100°C). The mixture was covered and allowed to steep for 10 minutes before filtration. The resulting infusions were stored in glass bottles, frozen, and lyophilized. For *P. barbatus*, *P. ornatus*, and *G. amygdalinum*, 100 g of fresh leaves were infused in 400 mL of boiling distilled water (100°C) for 10 minutes. After filtration, the aqueous extracts were immediately frozen at -80°C and subsequently lyophilized. All processed samples were labeled as detailed in Table I.

ESI-MS Analysis and Chemometric Processing

Mass spectral data were acquired using an LCQ Fleet ion trap mass spectrometer (Thermo Scientific) equipped with both electrospray ionization (ESI) and atmospheric-pressure chemical ionization (APCI) sources operating in positive and negative modes. Lyophilized extracts were dissolved in methanol at a concentration of 1 mg/mL and introduced via direct infusion. The ionization settings for APCI analysis were as follows: source voltage, 5 kV, discharge current, 5 µA; vaporizer temperature, 350°C; sheath gas pressure, 35 arbitrary unit (arb); ion sweep gas pressure, 0.0 arb; aux gas pressure, 15 arb; capillary temperature, 260°C; tube lens offset, 120 V; skimmer offset, 0 V. The ionization settings for ESI analysis were as follows: spray voltage, 5 kV; sheath gas, 9 arbitrary unit (arb); auxiliary gas, 3 arb; sweep gas, 0 arb; capillary temp, 260°C; capillary voltage, 26 V; tube lens, 125 V. For both, APCI and ESI analysis helium was used as collision gas, and the MS/MS spectra were obtained using collision energies ranging from 20 to 25%.

Raw spectra were processed using Xcalibur software (v2.7, Thermo Scientific). For chemometric analysis, APCI(+) mass spectral data were organized in a matrix (samples × *m/z* features) and processed using Chemoface (v1.6.1). Multivariate analysis included: Principal

Table I. Sample labels for fresh boldo and commercially acquired *P. boldus*.

Species label	Specifications	Origin	Coordinates	Herbarium registration number
CPB-1	*P. boldus*	Boldo-do-Chile, brand I, supermarket 1, Itacoatiara	3.1406098403185125 58.4421831441846	-
CPB-2	*P. boldus*	Boldo-do-Chile, brand II, supermarket 1, Itacoatiara	3.1406098403185125 58.4421831441846	-
CPB-3	*P. boldus*	Boldo-do-Chile, brand I, supermarket 1, Itacoatiara	3.1406098403185125 58.4421831441846	-
CPB-4	*P. boldus*	Boldo-do-Chile, city market, Itacoatiara	3.1362390404186637 58.439458019833644	-
CPB-5	*P. boldus*	Boldo-do-Chile, supermarket III, Itacoatiara	3.1397676676999287 60.02218561327861	-
CPB-6	*P. boldus*	Boldo-do-Chile, city market, Manaus	3.1401533259354224 60.020490457207046	-
CPBa	*P. barbatus* (*in natura*)	Tiradentes neighborhood, Itacoatiara	3.1427294165778417 58.431567060542754	4467
CPO	*P. ornatus* (*in natura*)	São Jorge neighborhood, Itacoatiara	3.142857150311584 58.43725266654359	4395
CGA	*G. amygdalinum* (*in natura*)	Tiradentes neighborhood, Itacoatiara	3.1427294165778417 58.431567060542754	4391

Component Analysis (PCA) of detected ions and Hierarchical Cluster Analysis (HCA) which employed Euclidean distance metric and the average linkage method of the three principal components (Da Silva et al. 2016).

Determination of Antioxidant Activity

The antioxidant capacity was evaluated based on the samples' ability to scavenge the stable 2,2-diphenyl-1-picrylhydrazyl (DPPH·) radical. A freshly prepared methanolic DPPH· solution

(0.039 mg/mL) with an absorbance of 0.70 ± 0.02 at 515 nm (R^2 = 0.99) was used for all assays. The reaction mixture consisted of 3.9 mL DPPH• solution combined with 100 µL of either methanol (control) or sample extract (1 mg/mL in methanol). After incubation in darkness (30 min), absorbance was measured at 515 nm using a UV-M51 spectrophotometer (Bel Photonics).

A Trolox (6-hydroxy-2,5,7,8-tetramethylchroman-2-carboxylic acid) standard curve (100-1500 µM) was established, yielding the linear regression equation: y = -0.0006x + 0.923 (R^2 = 0.9999). Results were expressed as µmol Trolox equivalents (TE) per gram of extract, derived from the standard curve.

Quantification of Total Phenolic Content

The total phenolic content was determined using an optimized Folin-Ciocalteu assay. Each sample (2 mg/mL in methanol) was added to a Folin-Ciocalteu reagent and sodium bicarbonate mixture (1:10 v/v) and allowed to incubate in darkness for 90 min at ambient temperature. Absorbance was measured at 725 nm using a spectrophotometer. Gallic acid was used as standard. Results were expressed as milligrams of gallic acid equivalents (GAE) per gram of sample.

In Silico Evaluation of Acetylcholinesterase (AChE) Inhibition via Molecular Docking

Molecular docking studies were conducted following an established protocol (Lima et al. 2019) with modifications. Phenolic compounds and alkaloids were retrieved from PubChem (https://pubchem.ncbi.nlm.nih.gov/) in SDF format; lowest-energy conformers were geometry-optimized using PM7 semi-empirical method (Stewart 2013); and energy minimization was performed with MOPAC2016 (Stewart 2016). The 3D crystal structure of *Torpedo californica* AChE (TcAChE) in complex with galantamine was obtained from RCSB Protein Data Bank (http://www.rcsb.org) (Bartolucci et al. 2001) under PDB ID 1QTI.

Docking was performed using the AutoDock Vina 1.1.2 software (Trott & Olson 2009) with the rid box centered on native ligand (x, y, z = 4.34, 64.37, 60.09). The search space size (grid box volume) was defined as 18 x 28 x 26 Å. Ligand and receptor conversion to PDBQT format was done via AutoDock Tools 1.5.6 (Morris et al. 2009). Discovery Studio Visualizer V16.1.0 (2016) was used for binding pose visualization and interaction analysis.

In Vitro Acetylcholinesterase (AChE) Inhibition Assay

AChE inhibitory activity was evaluated using an adapted Ellman's colorimetric method (Ellman et al. 1961). Concisely, neostigmine (1 mg) and AChE (10 µL) were prepared in phosphate buffer (1 mL) whereas the samples were prepared in MeOH (1 mL) and assessed at concentrations from 10 to 100 µg/mL. The assay was performed in triplicate using a 96-well microplate incubated in darkness during 15 min. Negative and positive controls were assessed under the same conditions. Absorbance was read ten times at a wavelength of 405 nm for 30 min with a 5-minute interval. The percentage of inhibition at each concentration was calculated according to the following equation:

$$\%\text{Inhibition} = A^2 - (A^1 - A^3) \times 100/A^2.$$

Where A^1 is the absorption of the sample and the enzyme, A^2 is the absorption of the enzyme without the sample, and A^3 is the sample absorption without the enzyme.

RESULTS

Chemical Profiling of Commercial *P. boldus* and *in Natura* Samples of *P. barbatus*, *P. ornatus*, and *G. amygdalinum*

Samples were botanically identified by analyzing stem characteristics (shape, color, surface texture, and additional structures) and comparing them with descriptions in virtual herbaria and taxonomic keys.

Direct infusion mass spectrometry was used to compare the chemical profiles of commercial *P. boldus* samples (Fig. 1) and *in natura* samples of *G. amygdalinum*, *P. barbatus*, and *P. ornatus* (Fig. 2).

Mass spectra analysis (positive mode) of the commercial *P. boldus* samples CPB2, CPB4, and CPB6 showed a base peak at *m/z* 342, consistent with alkaloids reported in *P. boldus* leaves. On the other hand, CPB5 exhibited a base peak ion at *m/z* 300, also indicative of alkaloids whereas CPB1 and CPB3 displayed distinct profiles, with prominent ions at *m/z* 365 and 445, suggesting compositional differences (Fig. 1). In order to tentatively identify key compounds (Fig. 2) in CPB2, CPB4, CPB5, and CPB6, the MS/MS spectra of selected ions were interpreted manually:

- *m/z* 342: fragments at *m/z* 311 (-31 Da, *m/z* 342 → 311), 296 (-15 Da, *m/z* 311 → 296), 279 (-32 Da, *m/z* 311 → 279), and 248 (-31 Da, *m/z* 279 → 248), suggest an aporphine alkaloid that have adjacent methoxyl groups at ring A and presence of *N*-methyl group, consistent

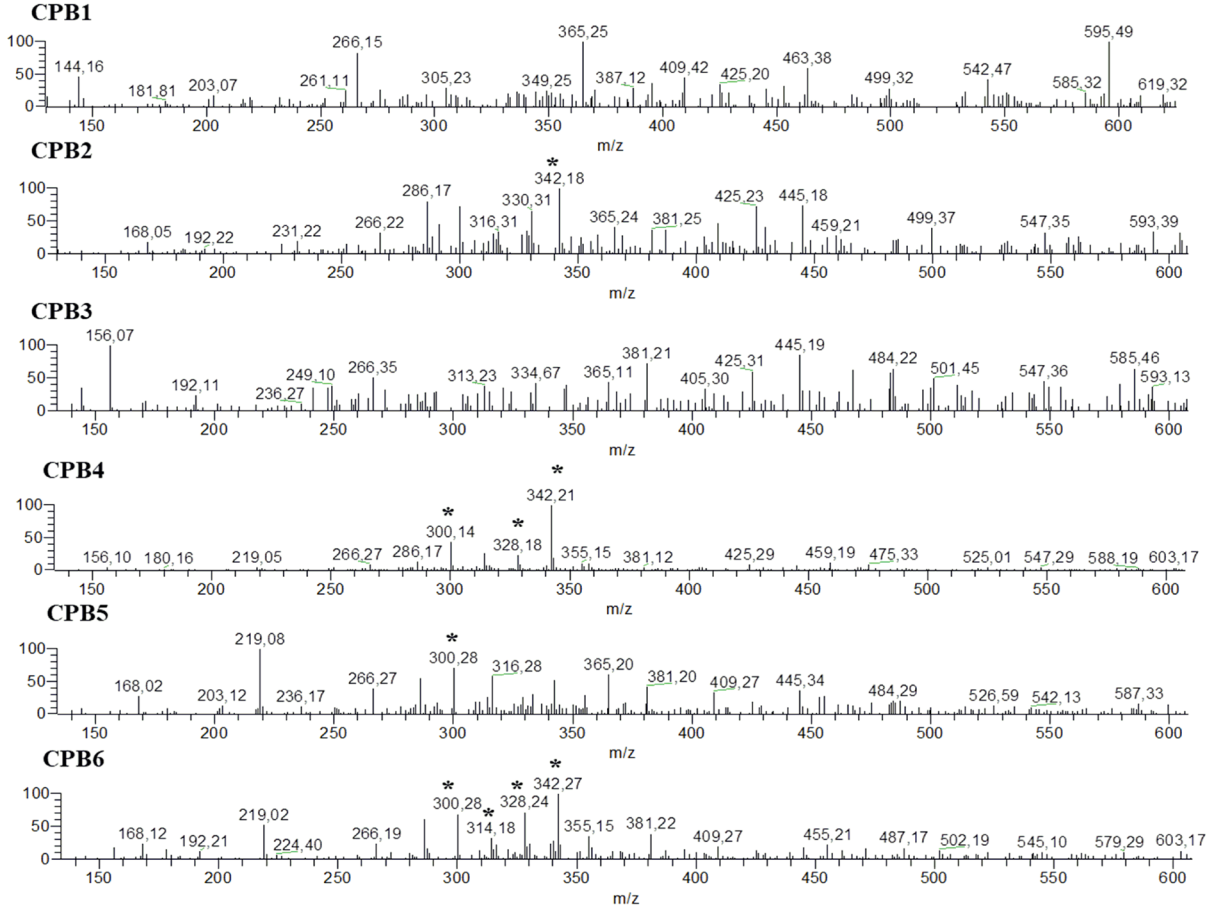

Figure 1. Mass spectra in positive mode of *P. boldus* samples.

with the alkaloid *N*-methyllaurotetanine, as reported in the literature (Falé et al. 2012, Torres-Vega et al. 2020, Da Silva et al. 2022);

- *m/z* 300: fragments at *m/z* 269, 237, 209, 192, 175, 145, 137, and 107. The initial loss of 31 Da (*m/z* 300 → 269), along with a diagnostic ion of benzylisoquinoline skeletons at *m/z* 107 is align with *N*-methylcoclaurine (Fig. 2a);
- *m/z* 328: fragments at *m/z* 297 (-31 Da, *m/z* 328 → 297), 265 (-32 Da, *m/z* 297 → 265), and 237 (-28 Da, *m/z* 265 → 237) suggest an aporphine alkaloids that have adjacent hydroxyl and methoxyl groups at ring A and the presence of *N*-methyl group, consistent with the alkaloid isoboldine;
- *m/z* 314: fragments at *m/z* 297 (-17 Da, *m/z* 314 → 297), *m/z* 265 (-32 Da, *m/z* 297 → 265), and 237 (-28 Da, *m/z* 265 → 237) are consistent with the alkaloid norisoboldine (Fig. 2 and Table II).

The CPB6 sample (*P. boldus*) was selected for comparison due to its characteristic ions (*m/z* 300, 328, 342) (Fig. 3a; Fig. 2; Table II). ESI-MS profiles of *P. boldus*, *G. amygdalinum*, *P. barbatus*, and *P. ornatus* revealed distinct chemical signatures (Fig. 3):

- *P. boldus*: dominant ions at *m/z* 342 and 328;
- *G. amygdalinum*: high-intensity ions at *m/z* 381;
- *P. barbatus*: prominent ion at *m/z* 485;
- *P. ornatus*: key ion at *m/z* 545.

Additionally, the above species shared minor ions: *m/z* 611 in the three *in natura*

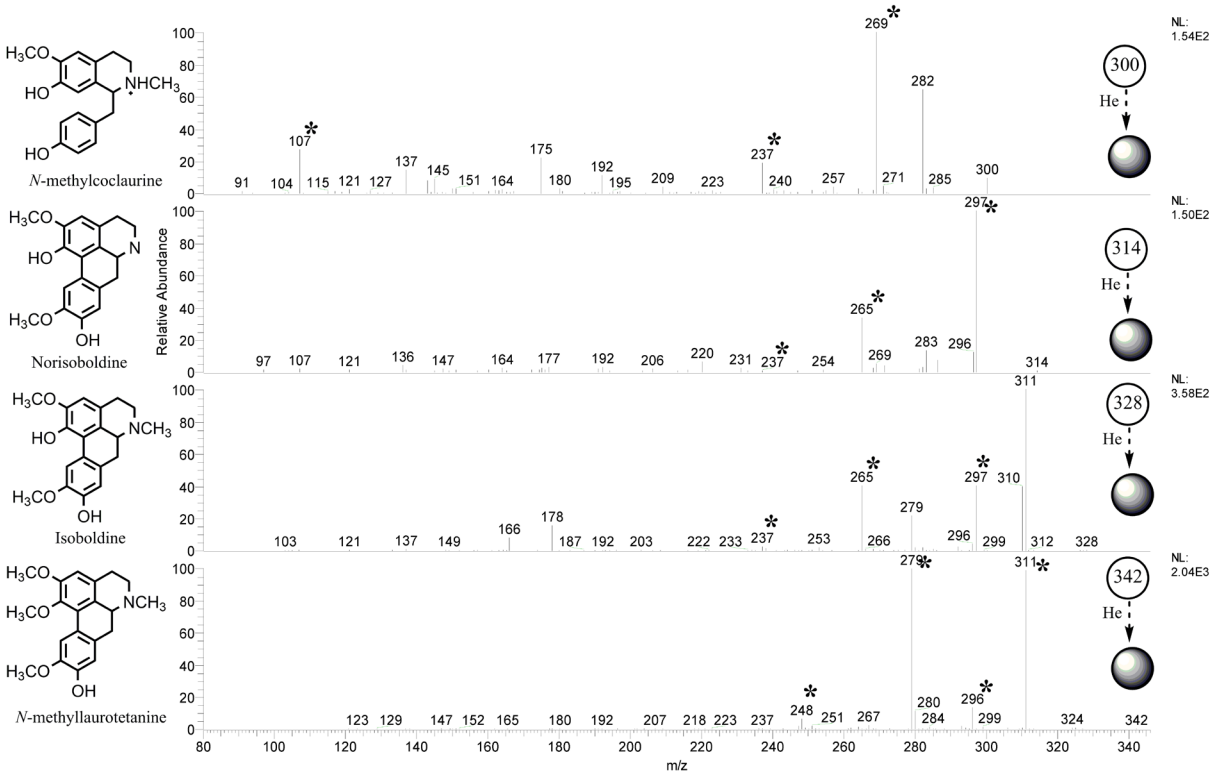

Figure 2. MS/MS spectra of the ions at m/z 300 (a), 314 (b), 328 (c), and 342 (d) of P. boldus samples. Ions marked with asterisk indicate fragment ions previously described in the literature for alkaloids *N*-methylcoclaurine, laurolitsine, isoboldine and *N*-methyllaurotetanine.

samples and *m/z* 567 in all four species (Fig. 3a, b, c, and d), indicating slight chemical overlap.

The PCA and HCA analyses of the chemical profile data enabled the grouping of the samples into three clusters (Fig. 4 and 5):

- Group I: *P. boldus* CPB1 (driven by *m/z* 708, 352, 139);
- Group II: *P. boldus* CPB3 (influenced by *m/z* 468);

Table II. Alkaloids tentatively identified in *P. boldus* (asterisk denotes base peak).

Sample	*m/z* precursor ion	Fragmented ions	Identification	Molecular formula	References
CPB2, CPB4, CPB5, and CPB6	300	269, 237, 209, 192, 175, 145, 137, 107	*N*-Methylcoclaurine	$C_{18}H_{21}NO_3$	Falé et al. 2012, Da Silva et al. 2022.
CPB3, CPB5, CPB6, CPB2, CPB1	328	297, 265, 237	Isoboldine	$C_{19}H_{21}NO_4$	Falé et al. 2012, Torres-Vega et al. 2020, Da Silva et al. 2022.
CPB2*, CPB4*, CPB6*, CPB5*	342	311, 296, 279, 248	*N*-Methyllaurotetanine	$C_{20}H_{23}NO_4$	Falé et al. 2012, Torres-Vega et al. 2020.
CPB2, CPB5, CPB6	314	297, 265, 237	norisoboldine	$C_{18}H_{19}NO_4$	Da Silva et al. 2022, Torres-Vega et al. 2020.

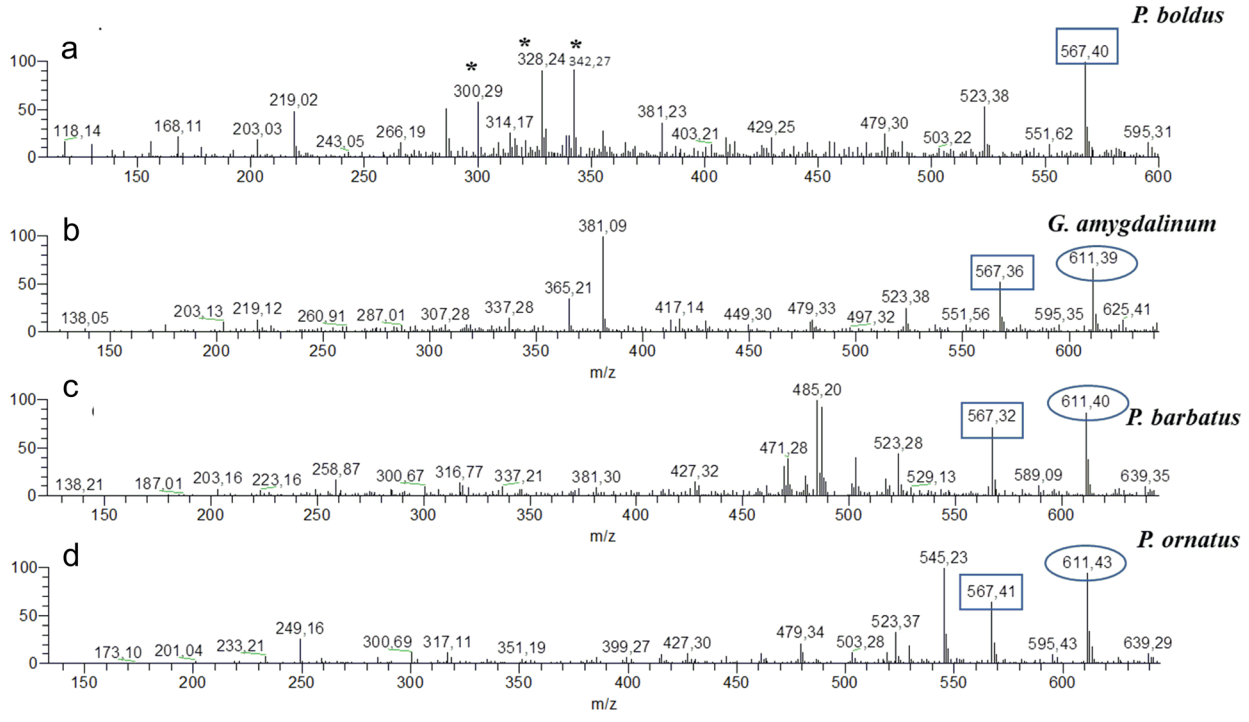

Figure 3. Mass spectra in positive mode of *P. boldus* (a), *G. amygdalinum* (b), *P. barbatus* (c), and *P. ornatus* (d). Ions circled in blue indicate the presence of ion *m/z* 611 in samples b, c, and d. The blue squares indicate the presence of ion *m/z* 567 in all samples.

- Group III: remaining *P. boldus* samples (CPB2, CPB4, CPB5, CPB6) and *in natura* samples of *P. barbatus*, *P. ornatus*, *G. amygdalinum*, (CPBa, CPO, CGA, respectively), linked by *m/z* 567 and 611.

CPB1 and CPB3 exhibited divergent profiles in line with the MS data (Fig. 1), suggesting potential misidentification as *P. boldus*. The HCA dendrogram in Figure 5 reinforced these groupings, with Group III further subdivided

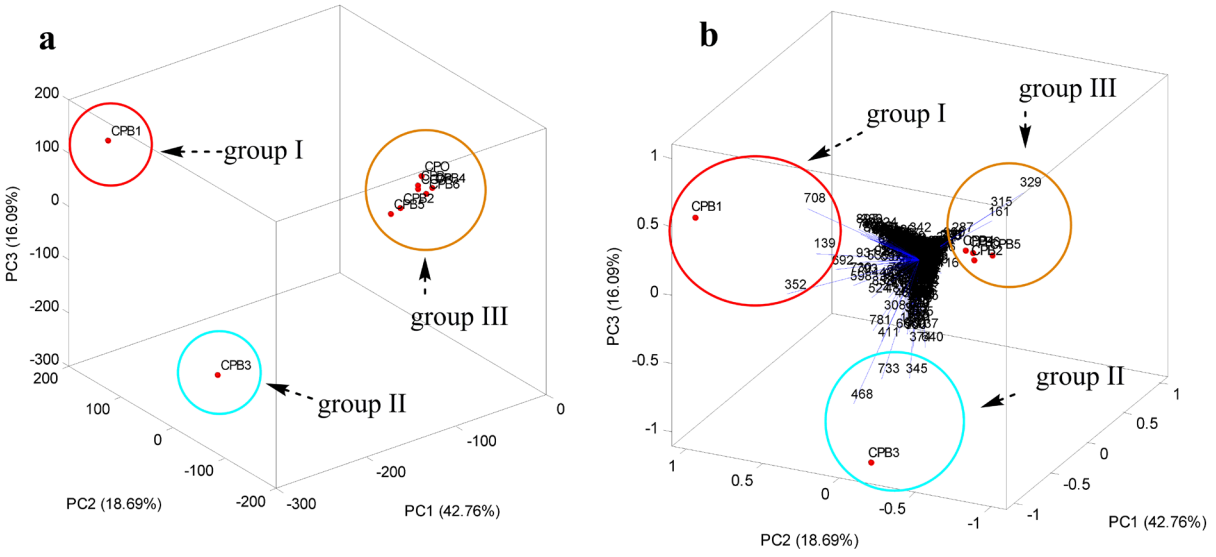

Figure 4. PCA score plot (a) and biplot (b) based on the chemical profile in positive mode APCI-MS.

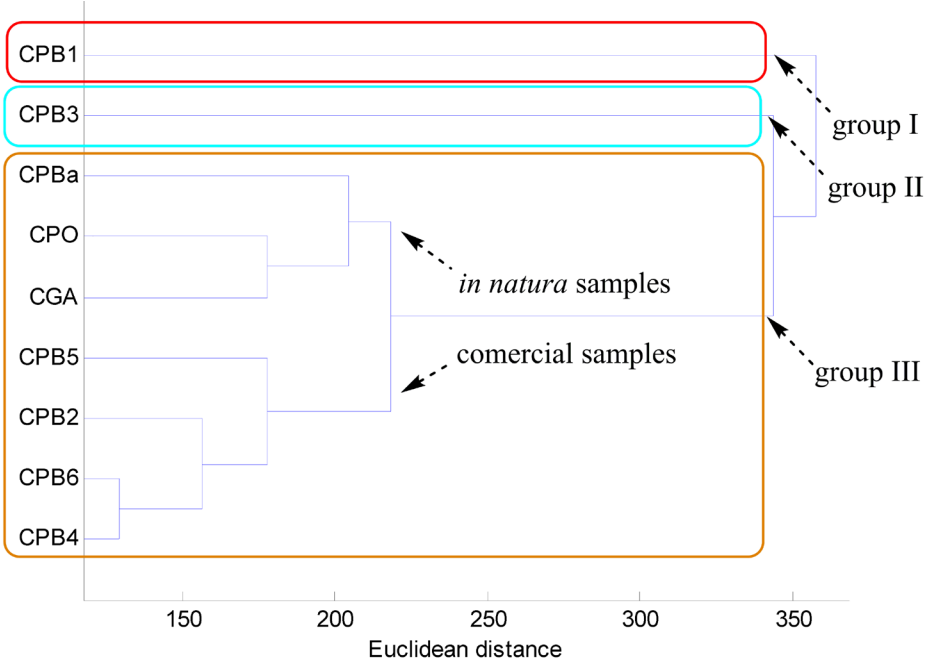

Figure 5. HCA dendrogram for commercial samples of *P. boldus* purchased at different venues (CPB1, 2, 3, 4, 5, and 6) and *in natura* samples of *P. barbatus*, *P. ornatus*, *G. amygdalinum* (CPBa, CPO, CGA).

into subgroups. High similarity was found among CPB2–CPB6, reflecting the chemical similarity seen in *P. barbatus*, *P. ornatus*, and *G. amygdalinum*. In addition, *P. ornatus* showed closer affinity to *G. amygdalinum* than to *P. barbatus*, a species of the same genus.

The APCI-MS analysis in negative mode (Fig. 6) enabled the identification of the following phenolic compounds:

- *P. barbatus*:
  - ◊ *m/z* 477: fragment at *m/z* 315 (-162 Da, *m/z* 477 → 315) is consistent with the flavonoid glycoside isorhamnetin 3-*O*-glucoside;
  - ◊ *m/z* 359: fragments at *m/z* 161, 179, 197 are consistent with rosmarinic acid (Hossain et al. 2010);
- *P. ornatus*:
  - ◊ *m/z* 463: fragments at *m/z* 301 (-162 Da, *m/z* 463 → 301) are consistent with the flavonoid glycoside quercetin 3-*O*-glucoside (Hossain et al. 2010);
  - ◊ *m/z* 421: fragments at *m/z* 343, 325, 307, 279, 273 are consistent with the diterpenoid coleon H, a compound frequently reported in *Plectranthus* species (Moser et al. 2023);
  - ◊ *m/z* 447: fragment at *m/z* 285 (-162 Da, *m/z* 447 → 285) is consistent with the flavonoid glycoside luteolin 7-*O*-glycoside;
- *G. amygdalinum*:
  - ◊ *m/z* 431: fragment at *m/z* 269 (-162 Da, *m/z* 431 → 269) is consistent with the flavonoid glycoside apigenin 7-*O*-glucoside (Tsakaris et al. 2022);
  - ◊ *m/z* 353: fragment at *m/z* 191 consistent with 3-*O*-caffeoylquinic acid (Gimenes et al. 2018).

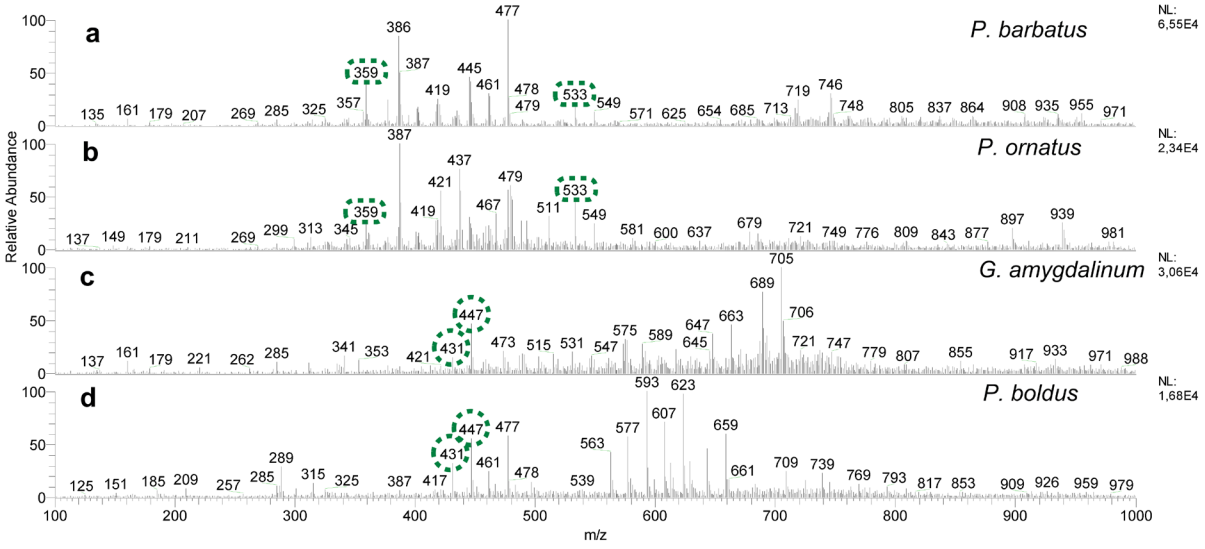

Figure 6. Mass spectra in negative mode of methanol fraction of *P. barbatus* (a), *P. ornatus* (b), *G. amygdalinum* (c), *P. boldus* (d) by APCI.

Table III. Total phenolic content and antioxidant activity of aqueous extracts of boldo species.

Species	Sample	TPC (mg EAG g^{-1})*	DPPH (μM ET)**
P. boldus	CPB6	305.32 ± 2.4	1073.33 ± 2.35
	CPB4	223.91 ± 0.8	1039.11 ± 88
	CBP2	219.09 ± 0.5	1068.33 ± 12.58
	CPB5	173.53 ± 1.7	1024.16 ± 1.17
G. amygdalinum	CGA	161.67 ± 4.8	457.22 ± 13.47
P. ornatus	CPO	88.05 ± 1.2	187.22 ± 34.25
P. barbatus	CPBA	167.71 ± 1.1	745.83 ± 24.74

*Milligrams of gallic acid equivalents per gram of sample. **Microliters of Trolox equivalents.

Total Phenolic Content and Antioxidant Activity

Total Phenolic Content (TPC)

The Folin-Ciocalteu assay revealed significant variation in phenolic content among the tested samples (Table III). Among commercial *P. boldus* extracts, CPB6 exhibited the highest TPC (305.32 mg GAE g^{-1}), exceeding both the other commercial samples (CPB2, CPB4, CPB5) and the *in natura* samples of *P. barbatus* (CPBa), *P. ornatus* (CPO), and *G. amygdalinum* (CGA): 167.71 ± 1.1 mg GAE g^{-1}; 161.67 ± 4.8 mg GAE g^{-1}; and 88.05 ± 1.2 mg GAE g^{-1}, in that order. Notably, all commercial *P. boldus* samples contained higher phenolic levels than those reported by Da Silva et al. (2022) for *P. boldus* aqueous extract (82.4 mg GAE g^{-1}).

Antioxidant Activity (DPPH Assay)

Antioxidant potential followed a similar trend. The commercial *P. boldus* samples exhibited high activity (1024.16 ± 1.17 to 1073.33 ± 2.35 μM ET), with no significant differences between them. Among the *in natura* samples, *P. barbatus* and *P. ornatus* exhibited the highest and the lowest antioxidant activity, respectively. *G. amygdalinum* (457.22 ± 13.47 μM ET) outperformed *P. ornatus*, aligning with its higher TPC. *P. ornatus* exhibited the lowest antioxidant capacity, consistent with its minimal phenolic content.

Molecular Docking Analysis

Molecular docking analysis of the major boldo-derived compounds with acetylcholinesterase (AChE) revealed strong binding interactions, with calculated binding energies ranging from -9.0 to -10.4 kcal/mol (Table IV). These values were comparable to that of the reference inhibitor galantamine (-10.3 kcal/mol), which was previously subjected to redocking validation (RMSD 0.3693 Å). Among the evaluated compounds, the flavonoid glycosides luteolin 7-*O*-glucoside and apigenin 7-*O*-glucoside exhibited the highest binding energies, with values of -10.4 and -10.3 kcal/mol, respectively.

In Vitro Assessment of Acetylcholinesterase Inhibition

The inhibitory activity of six boldo extracts against acetylcholinesterase (AChE) was evaluated, with all extracts demonstrating concentration-dependent inhibition (8.36-70.67 μg/mL). Among the tested compounds, boldine

Table IV. Result of molecular docking for the substances present in the extract of boldo species.

Species	Compounds	Binding Energy (kcal/mol)	Main interactions
Standard	Galantamine	-10.3	**HB** (Ser200, His440), **PAL** (Phe330), **PSI (**Trp84) **PP** (Phe331).
P. ornatus	Luteolin 7-*O*-glucoside	-10.4	**HB** (Gly118, Gly199, Glu199, Ser286, Phe288, Phe331, His440) **PP** (Trp279, Phe330).
G. amygdalinum	Apigenin 7-*O*-glucoside	-10.3	**HB** (Gly118, Gly199, Ser286), **PAL** (Ile287), **CH (**Ser200, His440) **PP** (Phe330).
P. boldus	*N*-Metillaurotetanine	-10.2	**HB** (Gln69), **CH (**Tyr70, Glu199, Phe330, His440), **PSI (**Trp84) **PP** (Phe331).
P. ornatus	Quercetin-3-*O*-glucoside	-10.1	**HB** (Trp84, Tyr121), **CH (**Gly118, His440), **PSI (**Trp84).
P. boldus	Isoboldine	-10.0	**HB** (Ser122), **PAL** (Phe330), **PSI (**Trp84) **CH (**Tyr70, Gly123, His440) **PP** (Phe331).
P. boldus	Norisoboldine	-9.9	**HB** (Trp84,Tyr121,Phe288,Arg289), **CH (**Asn85, Glu199) **PP** (Phe330).
P. barbatus	Isorhamnetin 3-*O*-glucoside	-9.8	**HB** (Tyr70, Asp72, Gly123), **CH (**His440) **PP** (Tyr121, Trp279, Phe330).
P. barbatus	Rosmarinic acid	-9.7	**HB** (Ser200), **CH (**Ser122) **PP** (Trp84), **PC** (His440).
G. amygdalinum	3-*O*-Caffeoylquinic acid	-9.0	**HB** (Tyr121, Ser122, Phe331), **CH (**Gly118) **PP** (Tyr334).

HB- hydrogen bond; PAL-π-alkyl; PSI-π-sigma; CH-carbon hydrogen bond; PP-π-π; PC- π-cation.

exhibited particularly potent inhibition (8.36 µg/mL), comparable to the reference standard neostigmine (Table V).

DISCUSSION

Electrospray ionization mass spectrometry (ESI-MS) analysis confirmed the identity of commercial 'boldo-do-Chile' samples (CPB2, CPB4, CPB5, CPB6) as *P. boldus* through detection of characteristic alkaloids (N-methyl-laurotetanine and laurotetanine), consistent with literature markers (Cassels et al. 2019). In contrast, CPB1 and CPB3 lacked these diagnostic alkaloids, suggesting potential quality issues or misidentification. Recent UHPLC-MS/MS data (Salehi et al. 2021) support that *N*-methyllaurotetanine—not boldine—is the predominant alkaloid in *P. boldus* leaves, aligning with pharmacopeial standards (Costa 2017).

Negative-mode MS analysis was required for *in natura* samples (*P. barbatus*, *P. ornatus*, *G. amygdalinum*), as their major phenolic components were not detectable in positive mode. Chemometric analyses revealed some chemical similarity among the four boldo species, consistent with their shared popular name and ethnomedicinal uses. These findings align with the mass spectrum results, which

Table V. Result of the action of the extracts of boldo species in inhibiting AChE.

Sample	IC_{50} (μg mL^{-1})	r^2
CPB1	58.12 (43.41-66.89)	0.8904
CPBA	60.30 (53.72-76.21)	0.9277
CGA	70.67 (63.09-81.79)	0.8985
CPO	43.55 (39.95-55.50)	0.9260
CPB3	70.59 (58.32-91.78)	0.9040
CPB4	56.91 (41.87-70.69)	0.8335
Boldine (standard)	8.36 (5.618-12.02)	0.9767
Neostigmine (standard)	1.154 (0.997-1.337)	0.9863

revealed slight chemical similarity among them. Notably, *G. amygdalinum* and *P. ornatus* clustered closely in HCA, corroborating prior reports of shared flavonoids (Santos 2022).

The high flavonoid content in these species reflects adaptive responses to high UV exposure, particularly for *P. barbatus*, *P. ornatus*, and *G. amygdalinum*, which are of African origin. Moreover, these *in natura* species were cultivated in Amazonas State near the equator, where year-round high solar exposure may enhance flavonoid production. In contrast to other boldo species, *P. boldus* is native to South America rather than Africa, where it has adapted to environments with significant UV exposure and climatic variability (Santos 2022).

The robust antioxidant activity exhibited by *P. boldus* correlated only partially with total phenolic content (TPC), implicating synergistic roles for alkaloids and phenolics. Quezada et al. (2004) identified flavonoids (44.1%) and alkaloids (15.6%) as the primary contributors to antioxidant activity, with catechin (60.9%) and boldine (35.6%) being the most active components. Similar results were reported by Lara-Fernández et al. (2013). These findings indicate that the therapeutic effects of *P. boldus* infusions derive not only from alkaloids like boldine, but also from diverse phenolic compounds with demonstrated antioxidant properties (Simirgiotis & Schmeda-Hirschmann 2010).

Unlike *P. boldus*, *Plectranthus* species (*P. barbatus*, *P. ornatus*) exhibited a direct correlation between antioxidant activity and total phenolic content (TPC), primarily mediated by rosmarinic acid and related phenolic compounds (Falé et al. 2009, Mendonça et al. 2023). For *G. amygdalinum*, antioxidant effects were principally associated with caffeoylquinic acids (Carvalho 2014), though potential contributions from saponins and sesquiterpene lactones (Unegbu et al. 2020) require additional investigation.

Our analysis revealed a general correlation between DPPH radical scavenging capacity and total phenolic content (TPC). However, *P. boldus* samples demonstrated consistently strong antioxidant activity regardless of TPC variations (CPB2-CPB6), suggesting contributions from both alkaloids and phenolic compounds, consistent with previous reports. In contrast, *Plectranthus* species (*P. barbatus* and *P. ornatus*; CPBa and CPO) showed a direct correlation between antioxidant activity and total phenolic content (Fig. 7), demonstrating phenolic-dependent free radical scavenging capacity.

Empirical studies demonstrate a robust correlation between DPPH radical scavenging activity and total phenolic content in *P.*

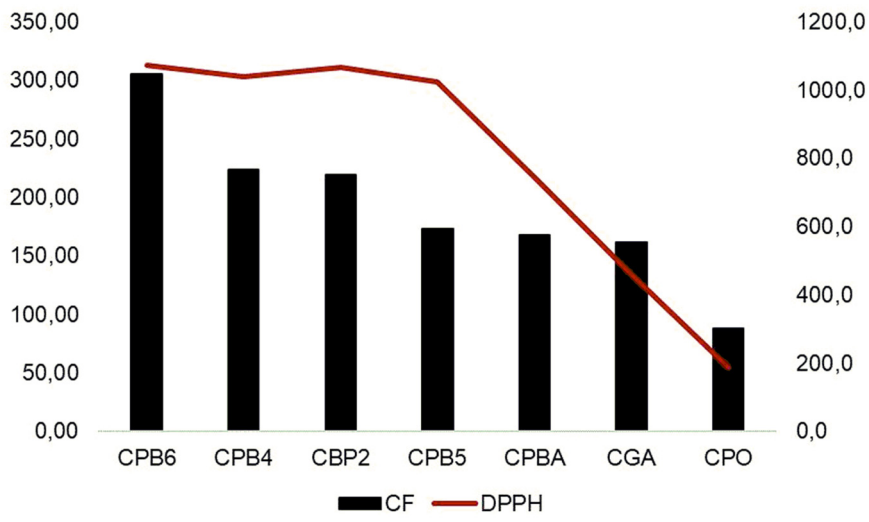

Figure 7. Relationship between total phenolic content and DPPH scavenging capacity.

barbatus extracts. Flavonoids, acids, esters, phenylpropanoids, and diterpenes, have been suggested to contribute to the antioxidant activity observed in the *Plectranthus* species. Rosmarinic acid—a characteristic component of *Lamiaceae* species—has been specifically implicated in antioxidant activity (Falé et al. 2009, Ganash & Qanash 2018, Mendonça et al. 2023).

Previous studies corroborate our findings regarding the antioxidant activity of *G. amygdalinum*. Da Silva et al. (2013) identified apigenin and luteolin as key flavonoid contributors, while Carvalho (2014) reported potent activity (EC_{50} = 20.0 ± 0.6 μg mL^{-1}) in leaf infusions, attributing this primarily to mono- and dicaffeoylquinic acids (e.g., chlorogenic acid and cynarin), via HPLC-MS analysis.

Our findings link the antioxidant activity of *G. amygdalinum* leaf infusions to its diverse phenolic compounds. However, contributions from other phytochemicals—including saponins, alkaloids, tannins, terpenes, and sesquiterpene lactones (Unegbu et al. 2020)—require further investigation.

Molecular docking studies were conducted using the AChE enzyme from *Torpedo californica* (PDB: 1QTI). This enzyme was selected due to its high sequence homology with human AChE and the availability of co-crystallized structures with well-established inhibitors such as galantamine, enabling reliable validation of the docking protocol. The enzyme's active site is located at the base of a deep gorge and is composed of several functional domains, including the catalytic triad (Ser200, His440, Glu327), which is essential for acetylcholine hydrolysis (Sussman et al. 1991), the anionic subsite (Trp84, Phe330), and the peripheral anionic site (Trp279), all of which are directly involved in ligand binding (Dvir et al. 2010).

To validate the docking protocol, a redocking study was performed by reintroducing galantamine into its original crystallographic position within the active site. The resulting root-mean-square deviation (RMSD) between the redocked and crystallographic poses was 0.3693 Å, confirming the accuracy and reliability of the predictive model. The interaction profile of galantamine (Fig. 8) was consistent with previous reports (Bartolucci et al. 2001), including hydrogen bonding between its methoxy group and the catalytic residues Ser200 and His440, as well as π–σ interactions with Trp84 and π–alkyl interactions with Phe330 within the anionic subsite.

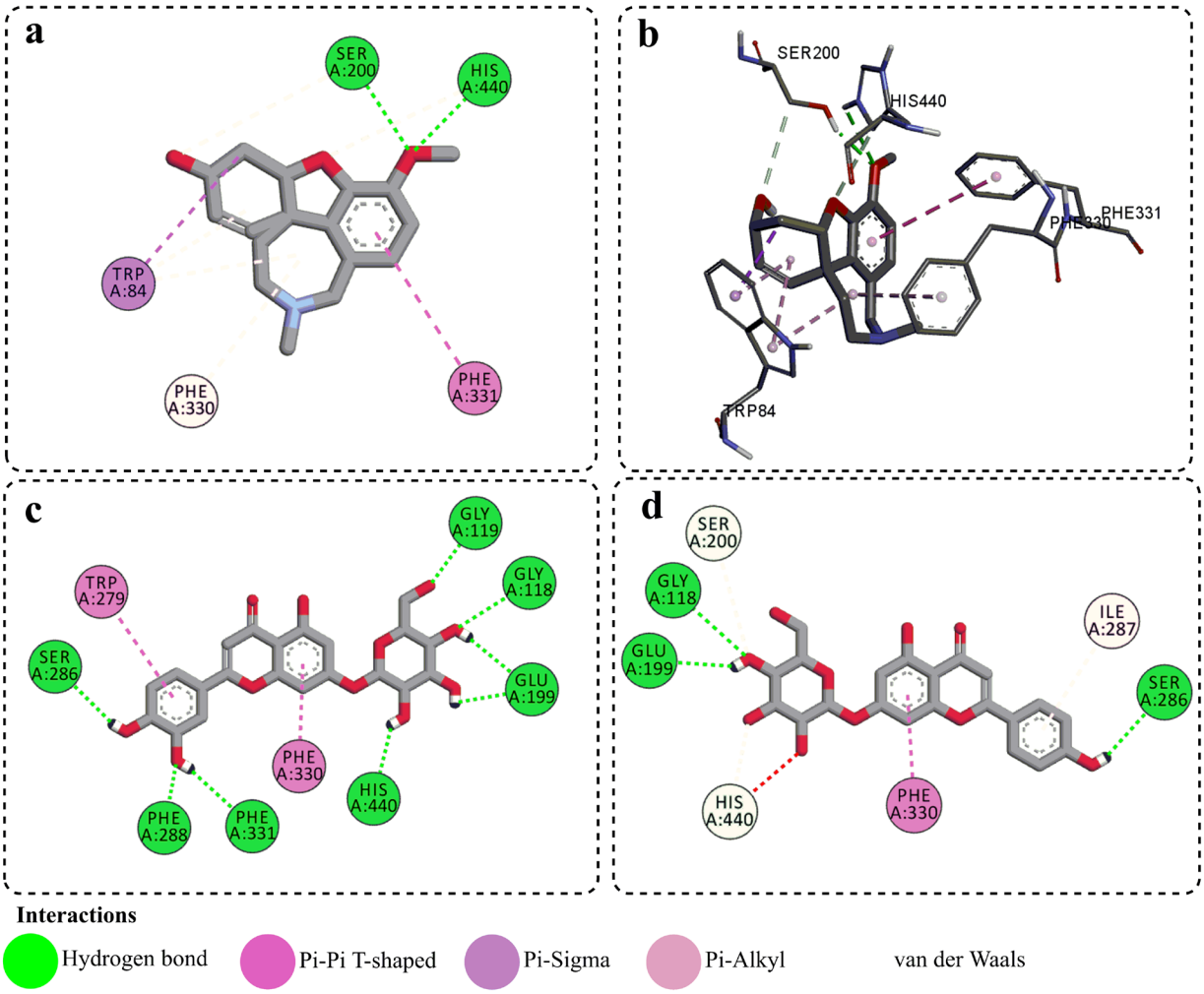

Figure 8. Main interactions identified for the galantamine-AChE complex in 2D (a) and 3D (b); Luteolin 7-*O*-glucoside-AChE (c) and apigenin 7-*O*-glucoside-AChE (d) complexes.

Among the tested compounds, flavonoid glycosides demonstrated the most favorable binding energies. Luteolin 7-*O*-glucoside (from *P. ornatus*, –10.4 kcal/mol) and apigenin 7-*O*-glucoside (from *G. amygdalinum*, –10.3 kcal/mol) showed stronger interactions with the enzyme's active site compared to the other compounds analyzed (Table IV). These binding affinities equaled or exceeded that of galantamine (–10.3 kcal/mol), a standard reference inhibitor of AChE in pharmacological studies (Jia et al. 2009, Marucci et al. 2021).

Luteolin 7-*O*-glucoside stood out by forming significant interactions with both catalytic and peripheral residues of the enzyme. It established hydrogen bonds with His440 and π–π stacking interactions with Trp279 and Phe330, indicating efficient insertion into both the catalytic and peripheral domains. In comparison, apigenin 7-*O*-glucoside exhibited a slightly less extensive interaction profile, yet still formed meaningful contacts with key residues of the catalytic triad, such as carbon–hydrogen bonds with Ser200 and His440, as well as interactions with Phe330. These findings suggest that apigenin 7-*O*-glucoside is also effectively accommodated within the active site of AChE (Dvir et al. 2010).

The inhibitory potential of flavonoid glyycosides against AChE has also been supported by other molecular docking studies. For instance, Mughal et al. (2018) evaluated a series of 3-*O*-flavonol glycosides and demonstrated that these compounds form stable interactions with the enzyme's active site, further confirmed through enzymatic inhibition assays. Similarly, flavanone glycosides such as naringin and hesperidin were investigated by Remya et al. (2014), showing high binding affinities toward AChE's active site through molecular docking analysis, with favorable interactions observed at critical residues.

CONCLUSIONS

Chemical profiling confirmed the authenticity of commercial 'boldo-do-Chile' samples CPB2, CPB4, CPB5, and CPB6 as *P. boldus* through detection of characteristic alkaloids (N-methyl-laurotetanine and laurotetanine). In contrast, CPB1 and CPB3 displayed divergent phytochemical profiles, suggesting misidentification or adulteration.

All investigated boldo species contained abundant phenolic compounds, correlating with their demonstrated antioxidant capacity. *In vitro* assays revealed moderate AChE inhibitory activity across species, while molecular docking identified promising candidates: flavonoids from *P. barbatus*, *P. ornatus*, and *G. amygdalinum*—which exhibited binding energies comparable to galantamine—and *P. boldus* alkaloids—which showed particularly high AChE affinity.

These findings position boldo species as valuable sources of neuroprotective agents through dual antioxidant/cholinesterase inhibitory activity, which makes them potential candidates for preventing and managing oxidative stress-related pathologies.

Acknowledgments

The authors are grateful to Programa de Pós-Graduação em Ciência e Tecnologia para Recursos Amazônicos (PPGCTRA – UFAM), EDITAL N. 003/2020 – PAINTER (process 01.02.016301.03897/2022-80) and EDITAL N. 008/2022 – KUNHÃ (process 01.02.016301.03977/2022-36) for the financial support.

REFERENCES

ALASBAHI RH & MELZIG MF. 2010. *Plectranthus barbatus*: A review of phytochemistry, ethnobotanical uses and pharmacology part 2. Planta Med 76: 753-765.

BARTOLUCCI C, PEROLA E, PIGLER C, FELS G & LAMBA D. 2001. Treedimensional structure of a complexo of galanthamine (Nivalin) with acetylcholinesterase from *Torpedo Californica*: implications for the desing of new anti-Alzheimer drugs. Proteins 42: 182-191.

CARVALHO AAAV. 2014. Estudo das atividades biológicas medicinais do extrato aquoso de vernonia condensata "boldo-baiano": inibição de acetilcolinesterase, atividade antioxidante, HMG-CoA redutase e biodisponibilidade de colesterol. Dissertação de mestrado. Universidade de Lisboa, Portugal, 81 p. (Unpublished).

CARVALHO RS ET AL. 2018. Antibacterial and antifungal activities of phenolic compound-enriched ethyl acetate fraction from *Cochlospermum regium* (mart. Et. Schr.) Pilger roots: Mechanisms of action and synergism with tannin and gallic acid. S Afr J Bot 114: 181-187.

CASSELS BK, FUENTES-BARROS G & CASTRO-SAAVEDRA S. 2019. Boldo, its secondary metabolites and their derivatives. Curr Tradit Med 5: 31-65.

COSTA FHM. 2017. Caracterização da composição química de extratos de boldos *in natura* e produtos comerciais derivados do boldo. Dissertação de Mestrado. Universidade Federal dos Vales do Jequitinhonha e Mucuri (UFVJM), Brasil, 62 p. (Unpublished).

DA SILVA BYK ET AL. 2022. Chemical and biological evaluation of the aqueous extract of *Peumus boldus* Molina (Monimiaceae) leaves. Pharmacogn Res 14: 45-52.

DA SILVA FMA ET AL. 2016. Chemical constituents from *Salacia impressifolia* (Miers) A C Smith collected at the Amazon rainforest. Biochem Syst Ecol 68: 77-80.

DA SILVA JB ET AL. 2013. *Vernonia condensata* Baker (Asteraceae): A promising source of antioxidants. Oxid Med Cell Longev 2013: 1-9.

DISCOVERY STUDIO VISUALIZER V16.1.0. 2016. Accelrys Inc., San Diego.

DVIR H, SILMAN I, HAREL M, ROSENBERRY TL & SUSSMAN JL. 2010. Acetylcholinesterase: from 3D structure to function. Chem Biol Interact 187: 10-22.

ELLMAN GL, COURTNEY KD, ANDRES V & FEATHERSTONE RM. 1961. A new and rapid colourimetric determination of acetylcholinesterase activity. Biochem Pharmacol 7: 88-95.

FALÉ PL, AMARAL F, AMORIM MADEIRA PJ, SOUSA SILVA M, FLORÊNCIO MH, FRAZÃO FN & SERRALHEIRO MLM. 2012. Acetylcholinesterase inhibition, antioxidant activity and toxicity of *Peumus boldus* water extracts on HeLa and Caco-2 cell lines. Food Chem Toxicol 50: 2656-2662.

FALÉ PL, BORGES C, MADEIRA PJA, ASCENSÃO L, ARAÚJO MEM, FLORÊNCIO MH & SERRALHEIRO MLM. 2009. Rosmarinic acid, scutellarein 4'-methyl ether 7-O-glucuronide and (16S)-coleon E are the main compounds responsible for the antiacetylcholinesterase and antioxidant activity in herbal tea of *Plectranthus barbatus* ("falso boldo"). Food Chem 114: 798-805.

FUENTES-BARROS G ET AL. 2023. Phytochemical variation of wild and farmed populations of boldo (*Peumus boldus* Molina). J Appl Res Med Aromat Plants 35: 100502.

GANASH M & QANASH S. 2018. Phenolic Acids and Biological Activities of *Coleus forskohlii* and *Plectranthus barbatus* as Traditional Medicinal Plants. Int J Pharmacol 14: 856-865.

GIMENES LP, AMARAL JG, MONGE M, SEMIR J, LOPES JLC, LOPES NP & BAUERMEISTER A. 2018. Phytochemical and chemotaxonomy investigation of polar crude extract from *Eremanthus incanus* (Asteraceae, Vernonieae). Biochem Syst Ecol 81: 105-108.

HOSALKOVA A ET AL. 2015. Alkaloids from *Peumus boldus* and their acetylcholinesterase, butyrylcholinesterase and prolyl oligopeptidase inhibition activity. Nat Prod Commun 10: 577-580.

HOSSAIN MB, RAI DK, BRUNTON NP, MARTIN-DIANA AN & BARRY-RYAN C. 2010. Characterization of phenolic composition in Lamiaceae spices by LC-ESI-MS/MS. J Agric Food Chem 58: 10576-10581.

ISHII T, MATAYOSHI N, TABA K & KAMADA T. 2022. Two new abietane diterpenoids from *Plectranthus barbatus*. Chem Nat Compd 58: 474-477.

JIA P, SHENG R, ZHANG J, FANG L, HE Q, YANG B & HU Y. 2009. Design, synthesis and evaluation of galanthamine derivatives as acetylcholinesterase inhibitors. Eur J Med Chem 44: 772-784.

LARA-FERNÁNDEZ L, RODRÍGUEZ-HERRERA R & AGUILAR CN. 2013. Separation conditions and evaluation of antioxidant properties of boldo (*Peumus boldus*) Extracts. J Med Plant Res 7: 911-917.

LIMA BR ET AL. 2019. Synthesis and inhibition evaluation of new benzyltetrahydroprotoberberine alkaloids designed as acetylcholinesterase inhibitors. Front Chem 7: 629.

LOPES ASN ET AL. 2020. Chemical composition and biological activities of the essential oil of *Peumus boldus* Molina (Monimiaceae). Rev Virtual Quim 12: 433-446.

MARUCCI G, BUCCIONI M, DAL BEN D, LAMBERTUCCI C, VOLPINI R & AMENTA F. 2021. Efficacy of acetylcholinesterase inhibitors in Alzheimer's disease. Neuropharmacology 190: 108352.

MENDONÇA SC, AAZZA S, CARVALHO AA DE, SILVA DM DA, OLIVEIRA N DE MS, PINTO JEBP & BERTOLUCCI SKV. 2023. Biological screening of herbal extracts and essential oil from *Plectranthus* species: α-amylase and 5-lipoxygenase inhibition and antioxidant and anti-Candida potentials. Braz J Pharm Sci 59: 1-16.

MORRIS GM, HUEY R, LINDSTROM W, SANNER MF, BELEW RK, GOODSELL DS & OLSON AJ. 2009. AutoDock4 and AutoDockTools4: Automated docking with selective receptor flexibility. J Comput Chem 30: 2785-2791.

MOSER JC, DA SILVA RCV, COSTA P, DA SILVA LM, CASSEMIRO NS, GASPAROTTO JUNIOR A, SILVA DB & DE SOUZA P. 2023. Role of K+ and Ca2+ Channels in the Vasodilator Effects of *Plectranthus barbatus* (Brazilian Boldo) in Hypertensive Rats. Cardiovasc Ther 2023: e9948707.

MUGHAL EU, JAVID A, SADIQ A, MURTAZA S, ZAFAR MN, KHAN BA & KHAN KM. 2018. Synthesis, structure-activity relationship and molecular docking studies of 3-*O*-flavonol glycosides as cholinesterase inhibitors. Bioorg Med Chem 26: 3696-3706.

OTERO C, MIRANDA-ROJAS S, LLANCALAHUÉN FM, FUENTES JA, ATALA C, GONZÁLEZ-SILVA G, VERDUGO D, SIERRA-ROSALES P, MORENO A & GORDILLO-FUENZALIDA F. 2022. Biochemical characterization of *Peumus boldus* fruits: Insights of its antioxidant properties through a theoretical approach. Food Chem 370: 131012.

QUEZADA N, ASENCIO M, VALLE JM, AGUILERA JM & GÓMEZ B. 2004. Antioxidant activity of crude extract, alkaloid fraction, and flavonoid fraction from boldo (*Peumus boldus* Molina) leaves. J Food Sci 69: 371-376.

REMYA C, DILEEP KV, TINTU I, VARIYAR EJ & SADASIVAN C. 2014. Flavanone glycosides as acetylcholinesterase inhibitors: computational and experimental evidence. Indian J Pharm Sci 76: 567.

SALEHI B ET AL. 2021. Ethnopharmacology, phytochemistry and biological activities of native chilean plants. Curr Pharm Des 27: 953-970.

SANTOS LP DOS. 2022. Estudo Farmacognostico Das Folhas De Cinco Plantas Medicinais Denominadas Por Boldo. Trabalho de Conclusão de Curso. Universidade Federal do Rio de Janeiro (UFRJ), Brasil, 59 p. (Unpublished).

SCHWANZ M, NUNES E, KONRATH EL, VENDRUSCOLO GS, SILVA MV DA, HENRIQUES AT & MENTZ LA. 2008. Caracterização farmacobotânica de *Peumus boldus* (Monimiaceae) e avaliação de atividades biológicas do alcalóide boldina. Lat Am J Pharm 27: 871-879.

SCHWANZ M. 2006. Desenvolvimento e Validação de Método Analítico para Quantificação da Boldina. Dissertação de Mestrado. Universidade Federal do Rio Grande do Sul (UFRGS), Brasil, 123 p. (Unpublished).

SILVA FMA, SILVA FILHO FA, LIMA BR, ALMEIDA RA, SOARES ER, KOOLEN HHF & et al. 2016. Chemotaxonomy of the amazonian *Unonopsis* species based on leaf alkaloid fingerprint direct infusion ESI-MS and chemometric analysis. J Braz Chem Soc 27: 599-604.

SIMIRGIOTIS MJ & SCHMEDA-HIRSCHMANN G. 2010. Direct identification of phenolic constituents in Boldo Folium (*Peumus boldus* Mol.) infusions by high-performance liquid chromatography with diode array detection and electrospray ionization tandem mass spectrometry. J Chromatogr A 1217: 443-449.

STEWART JJP. 2013. Optimization of parameters for semiempiricalmethods VI: more modificationstothe NDDO approximationsandre-optimizationofparameters. J Mol Model 19: 1-32.

STEWART JJP. 2016. MOPAC2016. Stewart Computational Chemistry, Colorado Springs, CO, USA.

SUSSMAN JL, HAREL M, FROLOW F, OEFNER C, GOLDMAN A, TOKER L & SILMAN I. 1991. Atomic structure of acetylcholinesterase from *Torpedo californica*: a prototypic acetylcholine-binding protein. Science 253: 872-879.

TORRES-VEGA J, GÓMEZ-ALONSO S, PÉREZ-NAVARRO J & PASTENE-NAVARRETE E. 2020. Green extraction of alkaloids and polyphenols from *Peumus boldus* leaves with natural deep eutectic solvents and profiling by HPLC-PDA-IT-MS/MS and HPLC-QTOF-MS/MS. Plants 9: 1-17.

TROTT O & OLSON AJ. 2009. Software news and update autodock vina: improving the speed and accuracy of docking with a new scoring function, efficient optimization, na multithreading. J Comput Chem 31: 455-461.

TSAKARIS AS, LOUCKOVA A, JAEGEROVA T, TOKAROVA V & HAJSLOVA J. 2022. The *in vitro* inhibitory effect of selected Asteraceae plants on pancreatic lipase followed by phenolic content identification through liquid chromatography high resolution mass spectrometry (LC-HRMS). Int J Mol Sci 23: 11204.

UNEGBU VN, NKWOEMEKA NE, OBUM-NNADI CN & OKEY-NDECHE FN. 2020. Phytochemical and antibacterial activities of *Vernonia amygdalina* leaves (bitter leaf) on two drug resistant bacteria. Int J Res Stud Microbiol Biotechnol 6: 30-37.

USUNOBUN U & NGOZI O. 2016. Phytochemical analysis and proximate composition of *Vernonia amygdalina*. Int J Sci World 4: 11-14.

JOSIELE V. GOMES[1]
https://orcid.org/0009-0007-3143-6623

ÍVINA T.M.TRINDADE[1]
https://orcid.org/0000-0002-2744-9583

RAFAELA R. DA SILVA[1]
https://orcid.org/0000-0002-4960-9736

BRUNA R. DE LIMA[2]
https://orcid.org/0000-0002-6481-9213

ANDRÉ C. DE OLIVEIRA[3]
https://orcid.org/0000-0001-9258-3108

FELIPE M.A. DA SILVA[4]
https://orcid.org/0000-0002-1809-1372

DOMINIQUE F.M. DO CARMO[1]
https://orcid.org/0000-0002-8835-1619

[1]Universidade Federal do Amazonas (UFAM), Instituto de Ciências Exatas e tecnologia (ICET), Av. Nossa Senhora do Rosário, 3863, 69100-021 Itacoatiara, AM, Brazil

[2]Universidade Federal do Amazonas (UFAM), Departamento de Química, Av. General Rodrigo Octavio Jordão Ramos, 1200, 69077-000 Manaus, AM, Brazil

[3]Instituto Nacional de Pesquisas da Amazônia (INPA), Laboratório de Malária e Dengue, Av. André Araújo, 2936, 69060-001 Manaus, AM, Brazil

[4]Instituto Nacional de Pesquisas do Amazônia (INPA), Coordenação de Tecnologia e Inovação, Av. André Araújo, 2936, 69060-001 Manaus, AM, Brazil

Correspondence to: **Dominique Fernandes de Moura do Carmo**
E-mail: dominiquefmc@ufam.edu.br

Author contributions

Dominique Fernandes de Moura do Carmo: conceptualization, methodology, writing – original draft preparation, supervision, review and editing, project administration, funding acquisition; Josiele Viana Gomes: sampling, laboratory analysis, data organization and validation, writing – original draft; Ívina Thayná Miranda Trindade: sampling, laboratory analysis, data organization; Rafaela Rolim da Silva: sampling, laboratory analysis, data organization and validation; Bruna Ribeiro de Lima: methodology, formal analysis, writing – original draft; André Correa de Oliveira: sampling, conceptualization; Felipe Moura Araújo da Silva: conceptualization, writing – review and editing.

How to cite

GOMES JV, TRINDADE ÍTM, DA SILVA RR, DE LIMA BR, DE OLIVEIRA AC, DA SILVA FMA & DO CARMO DFM. 2026. Chemical Profile, Chemometric Analysis, Acetylcholinesterase Inhibitory and Antioxidant Activity of Diverse Boldo Species Employed in The Amazon Region. An Acad Bras Cienc 98: e20250013. DOI 10.1590/0001-3765202620250013.

Manuscript received on January 14, 2025;
accepted for publication on August 2, 2025

Handling editor

Jailson de Andrade

Data availability

The authors confirm that the data supporting the findings of this study are available within the article. Further data are available from the corresponding author upon reasonable request.